The Electronic Properties of Cu_2ZnGeS_4, $Cu_2CdGeSe_4$, and $Cu_2CdSnSe_4$ Calculated by GGA+U Technique

Omehe N. N.
Federal University, Otuoke, Bayelsa State, Nigeria
omehenn@fuotuoke.edu.ng

D.O.I: 10.56201/ijccp.v9.no4.2023.pg100.114

Abstract

Cu_2ZnGeS_4, $Cu_2CdGeSe_4$, and $Cu_2CdSnSe_4$ crystallizes in the tetragonal (I-42m) stannite structure. Their electronic properties have been studied using the pseudopotential method within the framework of the density functional theory. For exchange and correlation, the GGA+U was used in conjunction with the projector augmented wave. The calculations predicted the three materials as semiconductors with indirect band gap value of 1.22 eV, 1.65 eV, and 1.92 eV for Cu_2ZnGeS_4, $Cu_2CdGeSe_4$, and $Cu_2CdSnSe_4$ respectively. The partial density of states calculations showed that for Cu_2ZnGeS_4 compound, Se-4p is the dominate state at the top of the valence band while Ge-4s is the principal state at the bottom of the conduction band. Similarly, the top of the valence band for $Cu_2CdGeSe_4$ is mainly of Ge-4s and Se-4p states while the bottom of the conduction band is populated mostly by Ge-3d and Ge-4p states. For $Cu_2CdSnSe_4$, VBM is composed mainly of Se-4p and CBM is composed of Se-5s and Cd-4d states.

Keywords: *Electronic structure, Semiconductor, GGA+U, Thermoelectric*

Introduction

Photonic devices harvest the energy of the sun, they have wide range of applications in Thermoelectric, Photodetectors, Photovoltaic cells, and Photocatalysis etc. This has made it increasingly important that new improved materials be sought. The quaternary chalcogenides are promising candidates for these applications. The series I-II-IV-VI compounds are earth abundant and are relatively cheap and non toxic. Cu_2ZnGeS_4, $Cu_2CdGeSe_4$, and $Cu_2CdSnSe_4$ are members of this series of compound. They have different phases which include Orthorhombic, Kesterite and Stannite. It has been proven that these materials are useful in solar cells (Kauk-Kuusik et al., 2018; Cheng et al., 2023), Photocatalysis of water (Guc et al., 2017), Thermoelectricity (Shi and Yin, 2013; Chetty et al., 2016; Wang et al., 20215; Fan et al., 2011; Liu et al., 2014), and Coolers (Wang et al., 2015).

Previous works reported in the literature include works by Moodie and Whitfield (1986). They studied two phases of Cu_2ZnGeS_4 using Convergent-Beam electron diffraction (CBED) and high-resolution Lattice imaging with 200 kv electrons. A stainnite structure with space group I-42m having lattice parameters a = 5.27 Å, and a Rhombohedial structure with lattice

parameters a = 36.6 Å, b= 655 Å and C = 7.52 Å were reported. Cu_2ZnGeS_4 has been prepared by the Bridgman technique. The samples were analyzed via variable angle spectroscopic ellipsometry, and finding on refractive index, absorption coefficient and reflectivity were reported (Leon et al, 2010). Levcenco et al, (2013), used Raman and Photoluminescence spectroscopy to study the optical and vibrational properties of Cu_2ZnGeS_4. Reactive magnetron co-sputtering technique has also been used to prepare samples of Cu_2ZnGeS_4, these samples were studied via Raman spectroscopy and x-ray diffraction, findings revealed that Cu_2ZnGeS_4 is tetragonal Stannite structured (Chen et al; 2014). The kesterite phase has been reported in the literature. Huang et al., (2015) also used the sulphurization of radio frequency magnetron sputtered precursor to prepare samples of Cu_2ZnGeS_4, and Cu_2ZnSnS_4, the thin films were analyzed and reported to be of the kesterite phase. The band gap reported for Cu_2ZnGeS_4 and Cu_2ZnSnS_4 are 1.98 eV and 1.54 eV respectively. Kohl et al., (2018), prepared samples of $Cu2(Zn,Ge)(S,Se)_4$ using thermal annealing of evaporated metallic precursors, their findings revealed a band gap of 1.45 eV and 2.0 eV respectively. Also, Schnabel et al., (2017), prepared samples of $Cu_2ZnGeS_xS_{4-x}$ using thermal annealing . The X-ray diffraction analysis revealed a kesterite phase. They studied the effect of varying the sulphur and selenium content on the band gap. A band gap range of 1.5 eV to 1.7 eV was reported. Another phase of Cu_2ZnGeS_4 reported in the literature is the orthorhombic structure with a band gap of 2.01 eV (Morales-Gallardo et al., 2021). A study on compositional variation was done by Chen et al., (2017), they varied the Tin (Sn) and Gemanium (Ge) content, and reported a band gap range of 1.04 eV to 2.16 eV, indicating that the band gap increases with increment of the Ge content. $Cu_2ZnGeSe_4$ films were prepared via sequential deposition on Mo coated Soda lime glass. The effect of precursor stack order, composition, and annealing temperature on the properties of $Cu_2ZnGeSe_4$ were studied. The value of the reported band gap is 1.5 eV (Buffiere etal., (2015). Shi et al., (2013) employed the solvothermal method in preparing samples of Cu_2ZnGeS_4 and $Cu_2ZnGeSe_4$ single crystalline nanowire arrays. Analyses were done using x-ray powder diffraction, energy dispersive x-ray spectroscopy and UV-vis spectrophotometer. Their findings showed that these materials are viable for photonic applications. The thermal evaporation technique was applied by Courel et al., (2018) in the growth of thin films of Cu_2ZnGeS_4. They studied the effect of Ge concentration in GeS precursor on the properties of the grown samples, they obtained a band gap range of 2.0 eV to 2.23 eV Bodner et al., (2022) also work on Cu_2ZnGeS_4 single crystals using chemical vapour transport reaction method, samples were prepared varying the temperature. A band gap range of 2.068 eV to 2.113 eV was reported. X-ray diffraction study carried out on sample grown by Agala et al., (2019) showed tetragonal structure with band gap of 1.8 eV. The effect of synthesizing temperature of $Cu_2CdGeSe_4$ crystals have been reported in the literature. Gulay at al., (2002) reported on the low and high temperature modifications of $Cu_2CdGeSe_4$, and these corresponds, to the stannite and orthorhombic phases respectively. Similarly, Krustok et al., (2019) reported a variation in band gap of $Cu_2CdGeSe_4$ crystals grown at different temperatures. Kauk –Kunsik et al., (2018), synthesized samples of $Cu_2CdGeSe_4$ by molten salt method. They used x-ray diffraction and Raman spectroscopy methods to analysis these samples, and reported two phases of $Cu_2CdGeSe_4$, the tetragonal and orthorhombic structure, the obtained band gaps are 1.14 eV and 1.27 eV respectively. The electronic properties of $Cu_2CdGeSe_4$ were reported by Ocheretova et al., (2015), they studied samples of $Cu_2CdGeSe_4$ via x-ray photoelectron spectroscopy (XPS) and x-ray emission spectroscopy. The effect of doping on the thermoelectric properties of $Cu_2CdGeSe_4$ have been reported. Wang et al., (2015) showed that

doping $Cu_2CdSnSe_4$ with Gallium (Ga) in moderate amount at the Tin (Sn) site improves thermoelectric performance. Also, Liu et al., (2014), doped $Cu_2CdSnSe_4$ with manganese (Mn) at the cadmium site to obtain samples of $CuCd_{1-x}Mn_xSnSe_4$ at moderate concentration of Mn, they reported an improvement in thermoelectric properties of the samples. Their DFT study showed a shift of the Fermi level into the valence band making the sample slightly metallic. Rincon et al., (2015) reported on the vibrational properties of $Cu_2CdSnSe_4$ via Raman study.

Some theoretical investigations based on DFT has been carried out on these materials under investigation. Chen et al., (2013) used the pseudopotential method to study the electronic and optical properties of Cu_2ZnGeX_4 (X = S, Se, and Te). They investigated the kesterite and the stannite phases of these materials. The full potential linearised augmented plane wave method (FP-LAPW) was utilized by Kodan et al., (2016) to study the electronic and optical properties of Cu_2ZnGeS_4, using for exchange and correlation, the generalized gradient approximation (GGA) and the modified Becke-Johnson (MBJ) potential, they reported and gaps of 0.5 eV for GGA and 1.2 eV for mBJ. Mesbahi et al., (2018) used FP-LAPW with GGA + TB –MBJ +U in their calculations to predict the properties of Cu_2ZnGeS_4, and reported a band gap of 2.0 eV for the Kesterite Phase. The Kesterite phase of $Cu_2CdSnSe_4$ was also studied by Hamdaoui et al., (2022) using (MBJ+U) technique. VU et al., (2019) also used MBJ+U to study the properties of $Cu_2CdSnSe_4$ and reported results comparable to experiment.

In this work, the GGA+U technique will be deployed to investigate the electronic properties of $Cu_2ZnGeSe_4$, $Cu_2CdSnSe_4$, and $Cu_2CdSnSe_4$.

Computational Details

Chalcogendes form a large series of structurally related materials. The tetragonal stannite structure is derived from Zinc-blende by doubling the lattice parameter in the c-direction and has the space group I-42m. There are two formula unit per unit cell and each anions (sulphur (S) and selenium (Se)) is surrounded by two group I (copper (Cu), one group II (zinc(Zn) and cadmium (Cd), and one group IV (Germanium (Ge) and Tin (Sn)). The Cu atom was assigned the 4d Wyckoff's atomic coordinate, Zn and Cd occupied the 2b Site. A total of 16 atoms was used per unit cell. The calculations were based on the density functional theory (DFT). The pseudopotential method implemented in the Abinit suite of software (Gonze et al.,2002; Gonze at al., 2005). The GGA +U technique was applied in computing the electronic band structure, total density of states (TDOS), and the partial density of states. The lattice parameters shown in table I and the atomic positions used in the calculations were adopted from Parasyuk at al, (2001); Gulay et al, (2022), and Olekseyuk et al., (2002). A tolerance of 10^{-10} was applied to the ground state calculations. An energy cutoff of 15 Ha and a k-point mesh of 256 was utilized. The following states were used in the projector augmented wave: Cu:3s,3p, 3d,4s Zn:3s,3p,3d,4s; Cd: 4d 5s; Sn: 4d,5s,5p; Ge:3d,4s,4p se: 4s, 4p.

Table1: Adopted input with references

	a(Å)	b(Å)	c(Å)
$Cu_2ZnGeSe_4$	5.6104[a]	5.6104[a]	11.0457[a]

$Cu_2CdGeSe_4$	5.7482[b]	5.7482[b]	11.0533[b]
$Cu_2CdSnSe_4$	5.6882[c]	5.6882[c]	11.3378[c]

[a]Parasyuk at al, (2001); [b]Gulay et al, (2022), [c]Olekseyuk et al., (2002)

Results and discussion

The electronic band structure of $Cu_2ZnGeSe_4$, $Cu_2CdGeSe_4$, and $Cu_2CdSnSe_4$ have been computed and the results are presented in Figures 1a to 1c respectively. The band structure is a plot of energy (eV) against high symmetry points in the irreducible brillouin Zone. The direction of plot is Γ-X-M-P-Γ-M. Figure 1a displays the electronic band structure of $Cu_2ZnGeSe_4$, and it predicts an indirect band gap value of 1.22 eV, which is in excellent agreement with experimental values (Chen et al, 2017; Buffiere et al; 2015) and previous theoretical work (Chen and Ravindra, 2013). The valence band maximum (VBM) occurred at the M-point of high symmetry while the conduction band minimum (CBM) is at the gamma point. The material is obviously a semiconductor as indicated by the existence of an energy band gap. The band structure is grouped into various subbands of varying energy width. The subband at the Fermi level in the valence band has a width of about 4.5 eV, while the subband in the conduction band minimum has a width of 0.8 eV. The bands at the vicinity of the Fermi energy are flat with narrow dispersion indicating several transition points in the band structure. Figure 1b displays the electronic band structure of $Cu_2CdSnSe_4$. The calculation predicted the material to be a semiconductor with an indirect band gap of 0.65 eV which is in fairly good agreement with reflectivity measurement of 1.22 eV (Krustok et al, 2019). The VBM is at the gamma point while CBM is between X and M point, like in $Cu_2ZnGeSe_4$ compound, the valence subband at the vicinity of the Fermi level has a width of 3.2 eV, which is 1.3 eV less than that of $Cu_2ZnGeSe_4$. The conduction subband at the conduction minimum has a width of 0.6 eV, again, this is less than what was calculated for $Cu_2ZnGeSe4$, but here, there are notable points along X-M direction and at the P point. Figure 1c is the band structure of $Cu_2CdSnSe_4$ predicted as a semiconductor with an indirect band gap of 1.92 eV. The width of the valence subband at the Fermi level is comparable to that of $Cu_2ZnGeSe_4$ with a value of about 4.0 eV. There is an upward shift of the conduction subband. The VBM is found at the M-Point while CBM is at the gamma point (Γ–Point).

(1a) (1b)

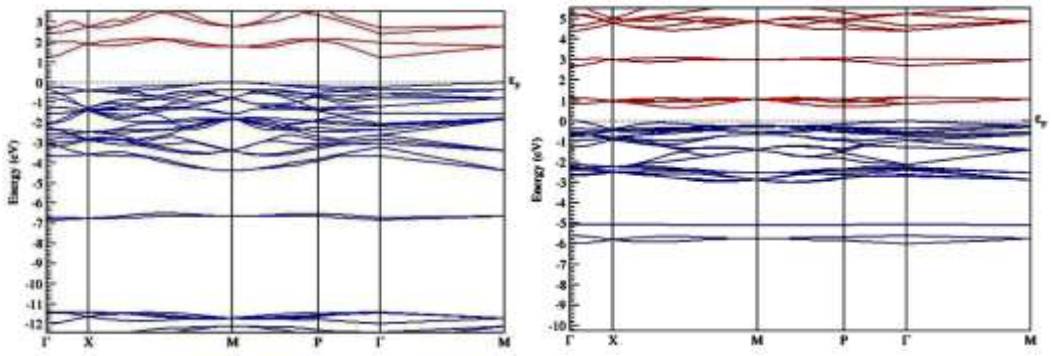

(1c)

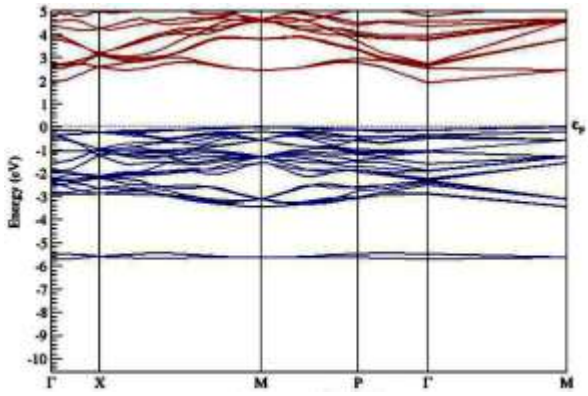

Figure 1: Electronic band structure of (1a) $Cu_2ZnGeSe_4$ (1b) $Cu_2CdGeSe_4$ and (1c) $Cu_2CdSnSe_4$.

The total density of states, (TDOS) for $Cu_2ZnGeSe_4$, $Cu_2CdGeSe_4$, and $Cu_2CdSnSe_4$ are presented in Figures 2a to 2c respectively. All features or subbands in the band structure are captured in the TDOS. The features or peaks represent the various orbital contribution to TDOS. In Figure 2a, the TDOS for $Cu_2ZnGeSe_4$ displayed. The Fermi level is at 0.1 Ha. The features from -0.1 Ha to 0.1 Ha is the valence subband while the feature about 0.2 Ha is the conduction band. For $Cu_2ZnGeSe4$, whose TDOS is displayed in figure 2b, the Fermi level is equally at 0.1 Ha. The reduced band gap of $Cu_2CdGeSe_4$ is obvious when compared to TDOS of $Cu_2ZnGeSe_4$ displayed in Figure 2a. The TDOS for $Cu_2CdSnSe_4$ is shown in Figure 2c, the features between - 0.1 Ha and 0.1 Ha is the valence subband at the Fermi level while that about 0.2 Ha represents conduction band. Like Figure 2a and 2b, the TDOS for $Cu_2CdSnSe_4$ captures all the subband in the band structure. The Fermi level is at 0.1 Ha and the band gap is seen between 0.2 Ha and 0.2 Ha. The feature between -0.1 to 1.Ha is the valence subband at the Fermi level while that about 0.2 Ha represents conduction band. Like in figure 2a and 2b, the TDOS for $Cu_2ZnGeSe4$ captures all the subbads in the band structure. The Fermi energy is at 0.1 ha and the band gap is seen between 0.1 and about 0.2 Ha.

(2c) (2b)

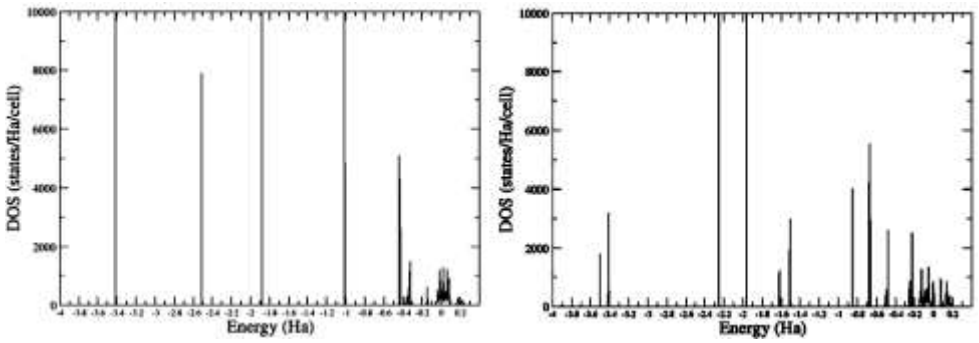

(2c)

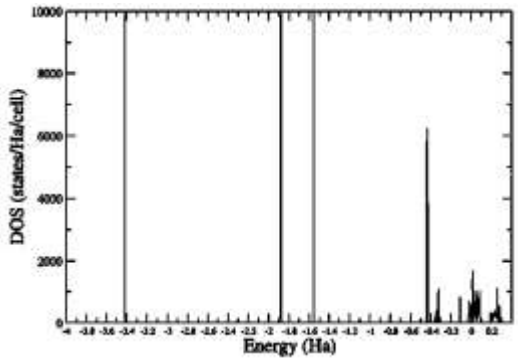

Figure2: The total density of states TDOS (2a) $Cu_2ZnGeSe_4$ (2b) $Cu_2CdGeSe_4$ and (3c) $Cu_2CdSnSe_4$.

The partial density of states (PDOS) for $Cu_2ZnGeSe_4$ is presented in Figures 3 to 6. PDOS is the orbital's contribution to the density of state (DOS) from all the constituent elements in the compound. Figure 3 is the PDOS for copper (Cu) atom. The Cu-3s, Cu-3p, Cu-3d and Cu-4s states are represented by the features in figure 3. The PDOS, like the TDOS, is a plot of DOS in (States/Ha/Call) against energy in Hartree (Ha). Cu-3s and Cu-4s are represented by the features in green, Cu-3s is the very narrow peak at -3.4 Ha, Cu-4s is the feature between -0.05 Ha to 0.1 Ha. There is also a small contribution of Cu-4s to the conduction band as seen about 0.2 Ha. The contribution of Cu-4s to the valence subband at the Fermi – level is quite small less than 20. The red peak at -1.9 Ha is the Cu-3p state. A small contribution from this state is also present at the valence band maximum. Cu-3d contribution is the feature in black and are the peaks between -0.5 to -0.3 Ha.

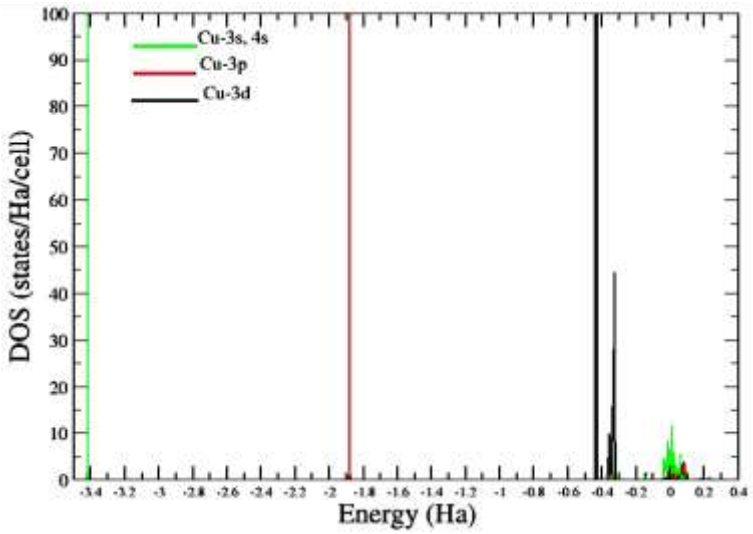

Figure 3: The PDOS of Cu orbitals in $Cu_2ZnGeSe_4$

Zinc's orbitals, Zn-3p, Zn-3d and Zn-4s are presented in Figure 4 by the red, black, and green features of the plot. The peaks like straight lines represent orbitals with very narrow or no dispersion. The narrow peak at -2.5 Ha is Zn -3p state, Zn-3d is at -1.0 Ha, these are states lower energy in the valence band, they are included in the PAW as semi core states. The valence

state, that is Zn-4s is the peaks in green and have higher energy levels, and the top valence band and conduction band are mostly of Zn-4s states.

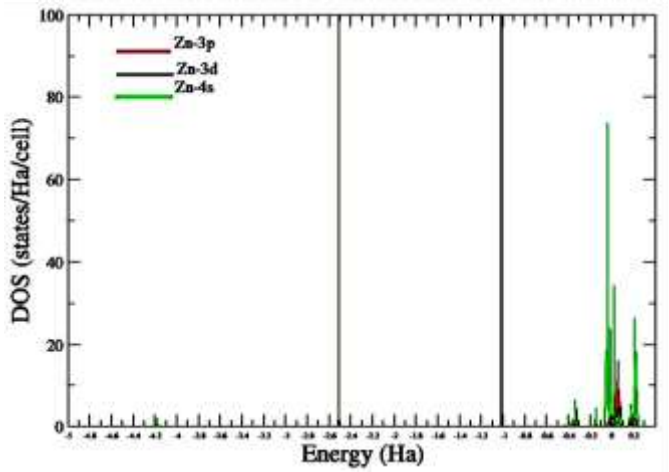

Figure 4: The PDOS of Zn orbitals in $Cu_2ZnGeSe_4$

Figure 5 is the orbital contribution of Ge, the states represented are Ge-4s, Ge-4p, and Ge-3d. the Ge-4s is represented by the green peaks between -0.4 and -0.3 Ha, the peak between -0.2 and -0.1 Ha and the peak at the conduction band minimum. The subband at the vicinity of the Fermi level is an overlap of Ge-4s, Ge-4p, and Ge -3d with Ge-3d dominating the top of the subband while the rear of the subband is majorly of Ge-4p. the states at the conduction band minimum is Ge-4s, though the three orbitals overlap in the conduction band.

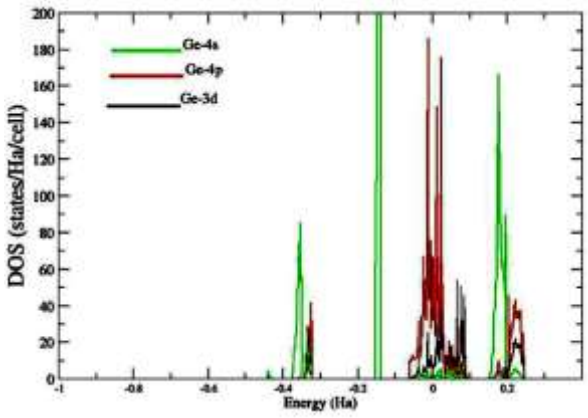

Figure 5: The PDOS of Ge orbitals in $Cu_2ZnGeSe_4$

Selenium's contribution is shown in Figure 6, and comes from Se-4s and Se-4p states. These state are represented by red and black features respectively. Se-4s is concentrated about -0.4 and -0.3 Ha. The subband preceding the band gap is dominantly Se-4p. In the electronic band

structure of $Cu_2ZnGeSe4$, Se-4p dominates the subband at the VBM while Ge-4s is the principal state at the CBM.

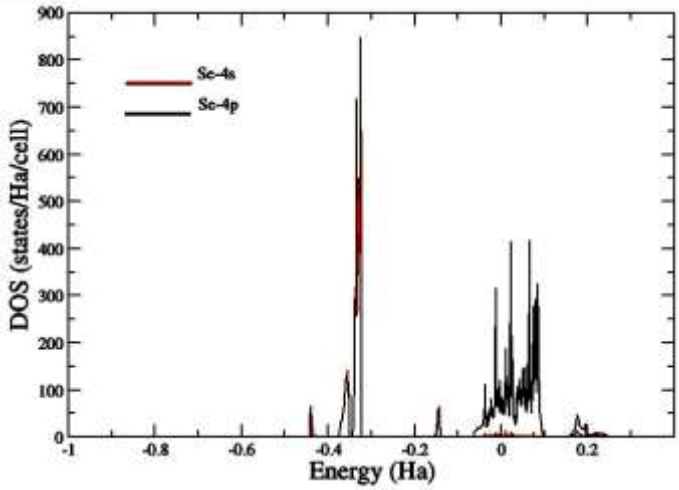

Figure 6: The PDOS of Se orbitals in $Cu_2ZnGeSe_4$

The orbital decomposition for $Cu_2ZnGeSe_4$ are presented in Figures 7 to 10. Cu-3s Cu-4s, Cu-3p, and Cu-3d state corresponds to the red, black, and green features of the PDOS in Figure 7. Cu's contribution to the subband at VBM and CBM are quite small, this is also comparable to Cu's contribuition to TDOS in $Cu_2ZnGeSe4$.

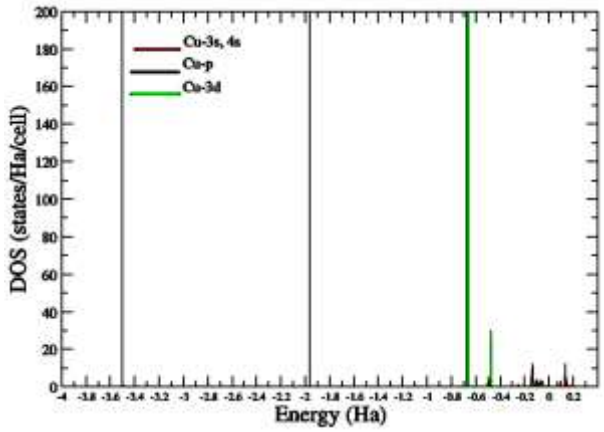

Figure 7: The PDOS of Cu orbitals in $Cu_2CdGeSe_4$

Figure 8 shows the contribution from Cd, its contribution comes from Cd-4d and Cd -5s orbitals. Most of Cd's contribution are of Cd-4d as seen from the red peaks.

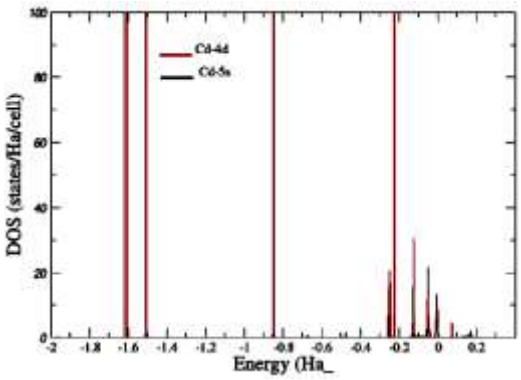

Figure 8: The PDOS of Cd orbitals in $Cu_2CdGeSe_4$

Figure 9 presented Ge contribution, again, this comes from Ge-3d, Ge-4s, and Ge-4p. these are represented by green, red, and black features of the graph. There is an overlaps of Ge-3d and Ge-4p in the CBN. The Ge-4s state dominates the top of the valence band.

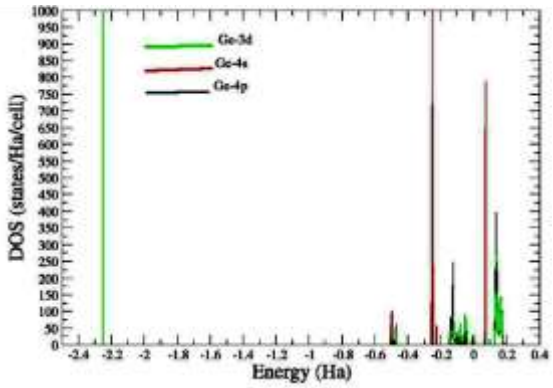

Figure 9: The PDOS of Ge orbitals in $Cu_2CdGeSe_4$

Selenium's contribution is shown in Figure 10, and this comes from Se-4s and Se-4p. The peak at -0.5 Ha is Se-4s contribution while the features about -0.1 and 0.1 are mainly Se-4p. So for $Cu_2ZnGeSe4$ compounds, its VBM is mainly of Ge-4s, Se-4p while CBM is mainly Ge-3d, Ge-4p.

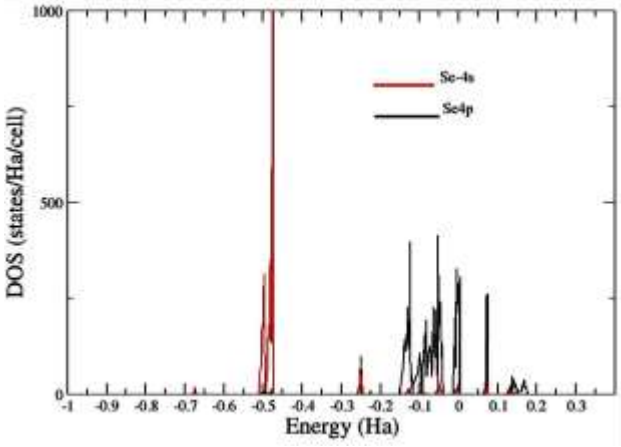

Figure 10: The PDOS of Se orbitals in $Cu_2CdGeSe_4$

PDOS for $Cu_2CdSnSe_4$ are presented in Figures 11 to 14. The black, green, and red features of Figure 11 are the states contribution from Cu-s, Cu-3p, and Cu-3d respectively. Cu-3s is the feature at -3.4 Ha, Cu-3p is represented by the peak at -1.9 Ha, Cu-3d about -0.42 and -0.2 .3 Ha. The Cu-4s contribution to VBM and CBM is small.

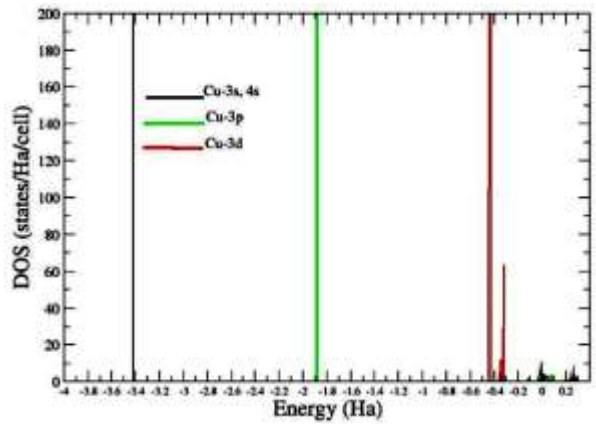

Figure 11: The PDOS of Cu orbitals in $Cu_2CdSnSe_4$

Figure 12 shows contribution from cadmium orbitals. Cd-4d and Cd-5s are shown in red and black respectively. Cd-4d dominates CBM and VBM Cd-5s dominate the rear of VBM subband.

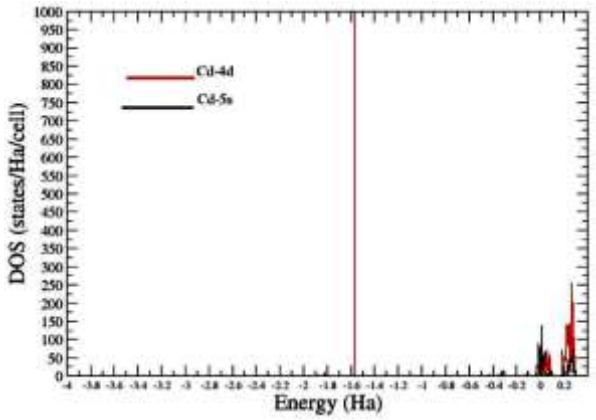

Figure 12: The PDOS of Cd orbitals in $Cu_2CdSnSe_4$

Tin's contribution is shown in Figure 13, and its orbitals Sn-4d, Sn-5p, and Sn-5s are depicted in red, green and black respectively. Sn-4d occupy the lowest energy level and is at -1.8 Ha. Sn-5s dominates CBM while Sn-5p dominates VBM.

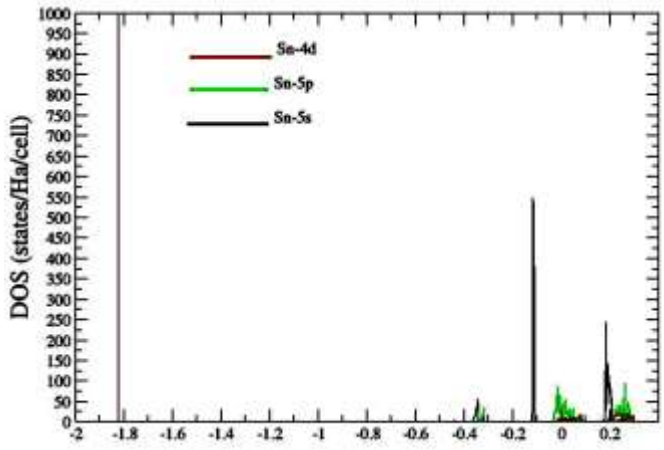

Figure 13: The PDOS of Sn orbitals in $Cu_2CdSnSe_4$

Selenium's contribution is shown in Figure 14. Se-4s and Se-4p features are in black and red respectively. Se-4s is the peak between -0.3 Ha and -0.4 Ha, while Se-4s is the state at the VBM subband. Se contribution to conduction band is from Se-4p States. For $Cu_2CdSnSe_4$ compound, VBM is composed mainly of Se-4p, and conduction band is mainly of Sn-5s and Cd-4d.

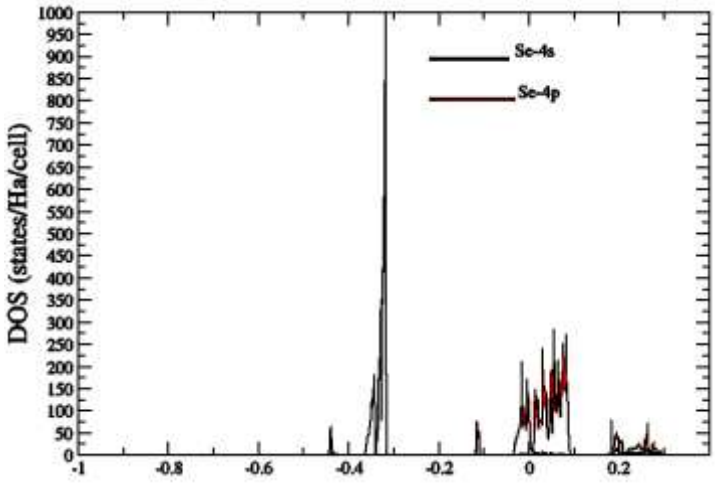

Figure 14: The PDOS ofSeu orbitals in $Cu_2CdSnSe_4$

Conclusion

Solar energy is clean and cheap, this is the driving force for the search for materials with high efficiency in conversion. A lot of experimental and theoretical studies have been done on the Quaternary compounds. It has been shown that these series of semiconductors are excellent solar absorbers. In this work, the electronic properties of Cu_2ZnGeS_4, $Cu_2CdGeSe_4$, and $Cu_2CdSnSe_4$ have been investigated via density functional theory. The results of the calculations showed that these materials are semiconductors wit indirect band gap.

References

Ayala A. M., Mathew N. R., Pal m., Gupta G. K., Dixit A., amd Mathew X. (2019), Facial synthesis of Cu_2ZnGeS_4 thin films from binary metal sulfides and study of their physical properties, Thin solid Films, 676, 30, 68-74.

Bodnar I. V, Yashchuk V. A. Pavlovskii V. N., and Yablonskii G.P. (2022), Growth, crystal structure and temperature dependence of the band gap of Cu_2ZnGeS_4 Single crystals, Semiconductors, Vol 56, No 5, (2022), 341-344.

Buiffiere M.; Elanzeery H., Souhaib O.; Messaoud K. B.; Bramertz G, Meuris M., Poortmans J. (2015), Physical characterization of $CuZnGeSe_4$ thin films from annealing of Cu-Zn-Ge precursor layers, Thin Solid films 582(1):171-175, DOI:10:1016/j.tsf.2014.09.024.

Chen D. and Ravindra N. M. (2013), Electronic and optical properties of Cu_2ZnGeX_4 (X=S,and Te) quaternally semiconductors, J. Alloys Compd. 579 (2013), 468-472.

Chen G., Wang W., Chen S., Whang Z., Huang Z., Zhang B., and Kong X. (2017), Bandgap engineering of $Cu_2ZnSn_{1-x}Ge_xS(e)_4$ adjusting Sn-Ge ratio for almost full solar spectrum absorption, J. Alloys compd. 718, pp 236-245.

Chen J., Zhao L., Liu F., Huang S., Hao S. (2014), Preparation and characterization of Cu_2ZnGeS_4 thin films by sulfurizing reactively sputtered precursors, 2014 conference on optoelectronic and microelectronic materials and devices, Perth, WA. Australia, 2014, pp 254-257, DOI:10.1109/Commad.2014.7038705.

Cheng N. Liu Z., Li W. Yu Z., Lei By Zi W., Xiao Z., Sun S, Zhao Z., Zong P-A. (2023), Cu_2ZnGeS_4 as a novel hole transport material for carbon-based perovskite solar cells with power conversion efficiency above 18%, Chemical engineering journal, vol. 454, part 1, https://doi.org/10.1016/;cej.2022.140146.

Chetty R., Bali A. and Malik R. C. (2016), Theormoelectric properties of indium doped $Cu_2CdGeSe_4$, Intermetallics 72:17-24, DOI: 10.1016/j.internet.2016.01.004.

Courel M, Sanchez T. G, Mathew N. R., and Mathew X. (2018), Cu_2ZnGeS_4 thin films deposited by thermal evaporation: the impact of Ge concentration on physical properties, J.Phys. D. Appl Phys 51, 095107.

Fan F-J, Yu B, Wang Y-X, Zhu Y-L, Liu X-J, Yu S-H, and Ren Z. (2011), Colloidal synthesis of Cu_2CdSnS_{e4} nanocrystals and Hot –Pressing to enhance the thermoelectric figure of merit, J. Am Chem. Soc. 133, 40, 15910-15913, https://doi.org/10.1021/ja207159j.

Gonze X., Beuken J.-M., Caracas R., Detraux F., Fuchs M., Rignanese G.-M., Sindic L., Verstraete M., Zerah G., Jollet F., Torrent M., Roy A., Mikami M., Ghosez Ph., Raty J.-Y., and Allan D.C., (2002) First-principles computation of material properties : the Abinit software project, Computational Materials Science 25, 478-492.

Gonze X., Rignanese G.-M., Verstraete M., Beuken J.-M., Pouillon Y., Caracas R., Jollet F., Torrent M., Zerah G., Mikami M., Ghosez Ph., Veithen M., Raty J.-Y., Olevano V.,

Bruneval F., Reining L., Godby R., Onida G., Hamann D. R., and Allan D. C., (2005) A brief Introduction to the Abinit software package. Z. Kristallogr. 220, 558-562.

Guc M., Lahdranta E. Hajdeu-Chicarosh E., Levcenko S., Shakhov M. A., Zakharchuk J., Arushanov E., and Lisunov K.G. (2017), Mechanisms of charge transfer and electronic properties of Cu_2ZnGeS_4 from investigations of the high–field magnetotransport, Sci. Rep. 7, 10685, https://doi.org/10.1038/s41598-017-10883-0.

Gulay L.D, Romanyuk Y. E. and Parasyuk O.U. (2012), Crystal structures of low and high temperature modifications of $Cu_2CdGeSe_4$, J. Alloys Compd. Vol.347, issues 1-2, pp 193-197, https://doi.org/10.1016/so925-8388(02)00790-9.

Hamdaoui J.E., Kria M. Lakaal K., El-Yadri M. Feddi E. M. Rejas C.P, Perez L.M, Diaz P., Mora-Ramos M. E. and Laroze D. (2022), Ab initio study of carrier mobility, thermodynamic and thermoelectric properties of kesterite Cu_2ZnGeS_4, Int. J. Mol. Sci-23(21), 12785 https://doi.org/10.3390/ijms232112785

Huang L., Deng H. M., He J., Chen L .L., Yang P. X., and Chu J. H. (2015), Study of structural and optical properties of Cu_2ZnGeS_4 and Cu_2ZnGeS_4 thin film synthesized by sulfurization of stacked material layers, Materials Science Forum, Vol 814, pp.44-48, https://doi.org/10.4028/www.scientific.net/msf.814.44.

Kauk-Kuusik M., Li x, Pilvet M, Timmo K. Grossbery M. Raadik T., Danilson M. Mikli V., Altosaar, Krustok J., and Raudoja J. (2018), Study of $Cu_2CdGeSe_4$ monograin powders synthesized by molten sort method for photovoltaic c applications, Thin solid Films, Vol. 666, 15-19.

Kodan N., Auluck S., and Mehto B.R. (2016), A DFT study of the electronic and optical properties of a photovoltaic arbsorber material Cu_2ZnGeS_4 using GGA and mBJ exchange correlation potentials, J. Alloys Compd. Vol. 675, pp 236-243.

Kohl T., Brammertz G.; Wild J., Neuwirth M, Meuris M., Poortmans J., and Vermang B. (2018), Fabrication of high band gap kesterite solar cell absorber materials for tanden applications, Thin Solid films 660, DOI:10:1016/j.tsf.2018.06.038.

Krustok J., Raadik T., Kaupmees R. and Mere A. (2019), Observation of band gap fluctuation and carrier localization in $Cu_2CdGeSe_4$, J. Phys D. Appl. Phys 52, 285102, Doi:10.1088/1361-6463/abiafd.

Leon M., Levcenko S., Serna R., Guireva G., Nateprov A, Merino J. M., Friendrich E. J. Fillat U., Shorr S., Arushanov E. (2010), Optical constant of Cu_2ZnGeS_4 bulk crystals, J. Appl. Phys.108,0935002, https://doi.org/10.1063/1.3500439.

Levcenco S., GuC, M., Mershjann C, Gurieva G., Shorr S., Lux-steiner M., Arushanov E. (2013), Photoluminescence characterization of Cu_2ZnGeS_4 single crystals, Physica status solidi C, Vol. 10, issue 7-8 P.1079-1081, https://doi.org.1002/Pssc.

Liu F.S, Zheng J. X, Huang M.J, He.L.P.Ao W. Q, Pan F., and Li J.Q. (2014), Enhanced thermoelectric performance of $Cu_2CdSnSe_4$ by Mn doping: experimental and first principle studies, Scientific reports 4,5774, DOI:101088/srepo5774.

Meshahi M., Serdouk F., and Benkhedir M.L. (2018), A DFT study of the electronic and optical properties of kesterite phase of Cu_2ZnGeS_4 using GGA, TB-MBJ, and U exchange correlation potential, Acta Physica Polonica A, Vol 134.

Moodie A.F and whifield (1986), Determination of the structure of Cu_2ZnGeS_4 polymorph by lattice imaging and covergent beam electron diffraction, Acta. Cyst. (1986). B42, 236-247, https://doi.org/10.1107/So1087 68160982

Morales-Gallardo M.V, Mathews N. R., Pal M., and Delgado F.P. (2021), Cu_2ZnGeS_4 nanorods by solvottermal method: Physical and Photocatalytic properties, J. Mater Sci: Mater Electron 32, 17282-17291, https://doi.org/10.1007/s10854-021-06232-7.

Ocheretova V.A, Parasyuk O.V, Kyyzhun O.Y. (2015), Electronic structure of $Cu_2CdGeSe_4$ single crystal as determined from x-ray spectroscopy data, Mater Chem Phys., Vol. 160, 345-351.

Olekseyuk I.D, Gulay C.D, Parasyuk O.V, Piskach L.V, Dydchak I.V., Marchuk O.V. (2002), Single crystal preparation and crystal structure of the (Cu2Zn)/(Cd,Hg)/(SnSey) compounds, J. Alloys Compd. , 340,141-145.

Parasyuk O.V, Romanguk Ya E. Gulay L.D, Piskach L. D. (2001), Phase diagram of the Cu_2GeSe_3-ZnSe System and Crystal structure of the $Cu_2ZnGe\ Se_4$ compound, J. Alloys compd, 329, 202-207.

Rinco C., Quintero M, Moreno E, Martinex J. A. H, Macias M.A. (2015), Raman spectrum of $Cu_2CdGeSe_4$ stannite structure semiconductor compound, Superlattices and Microstructures, 88: 99-103, DOI: 10.10/j.spmi.2015.08.032.

Schnabel T., Sebou M., and Ahlswede E. (2017), Band Gap Tuning of $Cu_2ZnGeS_xSe_{4-x}$ Absorsbers for Thin-Film solar cells, Energies 10 (11):1813, DOI:10.3390/en/0111813.

Shi L. and Yin P. (2015), Phosphate-free synthesis, optical absorption and photoelectric properties Cu_2ZnGeS_4 and Cu_2ZnGeS_4 uniform nanocrystal, Dalton Trans. 42 (37), 13607-11, DOI:10.1039/C3dt50993a.

Shi L.; Yin P., Zhu A., and Li Q. (2013), Synthesis and photo electric properties of Cu_2ZnGeS_4 and $Cu_2ZnGeSe_4$ single crystalline Nanowire Arrays, Langmuir 29, 27, 8713-8717, https://doi.org/10.1021/ia401531r

Vu T. V. lavrenty A. A., Gabralian 13.V., Pham K. D., Nguyen C. V. Trans K. C., Luong H.L, Batouche M., Parasyuk O.V and Khyzhun. (2019), Electronic, Optical and Elastic properties of $Cu_2CdGeSe_4$.: A first principles study, J.Electron Mater 48, 705-715, https://doi,org/`0.1007/s//664-018-6781-9.

Wang B., L. Y, Zhang J. XU M., Liu F., Ao W., L. J., and Pan F. (2015), Heterovalent substitution to enrich electrical conductivity in $Cu_2CdSn_{1-x}Ga_xSe_4$ series for high thermoelectric performance, Scientific reports 5, 9365, DOI: 10.1038/srepo9365.